COMM. MATH. SCI.
Vol. 1, No. 4, pp. 809–828

EFFECTIVE ONE PARTICLE QUANTUM DYNAMICS OF ELECTRONS: A NUMERICAL STUDY OF THE SCHRÖDINGER-POISSON-Xα MODEL*

WEIZHU BAO †, N.J. MAUSER‡, AND H.P. STIMMING §

Abstract. The Schrödinger-Poisson-Xα (S-P-Xα) model is a "local one particle approximation" of the time dependent Hartree-Fock equations. It describes the time evolution of electrons in a quantum model respecting the Pauli principle in an approximate fashion which yields an effective potential that is the difference of the nonlocal Coulomb potential and the third root of the local density. We sketch the formal derivation, existence and uniqueness analysis of the S-P-Xα model with/without an external potential.

In this paper we deal with numerical simulations based on a time-splitting spectral method, which was used and studied recently for the nonlinear Schrödinger (NLS) equation in the semi-classical regime and shows much better spatial and temporal resolution than finite difference methods. Extensive numerical results of position density and Wigner measures in 1d, 2d and 3d for the S-P-Xα model with/without an external potential are presented. These results give an insight to understand the interplay between the nonlocal ("weak") and the local ("strong") nonlinearity.

1. Introduction

One of the fundamental tasks of many body quantum mechanics is the approximation of "exact" N body problems by simpler models, in particular "one body" equations. The linear Schrödinger equation for the wave function $\Psi = \Psi(\mathbf{x}_1, \mathbf{x}_2, ..., \mathbf{x}_N, t)$ of N electrons interacting via the Coulomb potential reads

$$i\varepsilon\partial_t\Psi = -\frac{\varepsilon^2}{2}\sum_{j=1}^{N}\Delta_{\mathbf{x}_j}\Psi + \sum_{1\le j\le N}\sum_{j<k\le N}\frac{C}{|\mathbf{x}_j-\mathbf{x}_k|}\Psi\,, \qquad t\in I\!R, \tag{1.1}$$

$$\Psi(\mathbf{x}_1,\cdots,\mathbf{x}_N,t=0) = \Psi_I(\mathbf{x}_1,\cdots,\mathbf{x}_N)\,, \qquad \mathbf{x}_j\in I\!R^d, \quad j=1,\cdots,N\,. \tag{1.2}$$

Here $\varepsilon \simeq \hbar$ stands for the scaled Planck constant, which we will consider as a small, tunable parameter, i.e. $0 < \varepsilon \ll 1$, the mass and other physical constants are kept fixed and scaled to 1.

A successful method to rigorously derive "mean field approximations" and other nonlocal "one particle" Schrödinger equations from (1.1) is "weak interaction limits" (see e.g. [BaG]), i.e. a limit where the number of particles N tends to infinity and the interaction potential among the particles is rescaled with $1/N$.

Depending on the "ansatz" for the (initial) N particle wave function Ψ_I, different asymptotic limits of the linear N particle Schrödinger equation are obtained: The "Hartree ansatz" $\Psi_I(\mathbf{x}_1,\cdots,\mathbf{x}_N) = \Pi_{k=1}^N\psi(\mathbf{x}_k)$ yields the Schrödinger-Poisson (S-P) equation for ψ. Even for this simplest approximation of (1.1) only recently rigorous derivations have been given in the time dependent case [BMY].

A serious drawback of the S-P model, i.e. the underlying Hartree ansatz, is that it does not respect the "Pauli exclusion principle" for fermions, hence the "exchange effects" of electrons are missing. These effects are taken into account by anti-

*Received: December 26, 2002; accepted (in revised version): October 24, 2003. Communicated by Shi Jin.

†Department of Computational Science, National University of Singapore, Singapore 117543.

‡Wolfgang Pauli Institute, c/o Inst. f. Mathematik, Univ. Wien, Strudlhofg. 4, A–1090 Wien, Austria.

§Wolfgang Pauli Institute, c/o Inst. f. Mathematik, Univ. Wien, Strudlhofg. 4, A–1090 Wien, Austria.

symmetrization of the N-particle wave function, as it is realized in the "Hartree-Fock ansatz".

In the sequel we sketch the derivation of the $X\alpha$ term for the stationary case: the starting point are the time-independent Hartree-Fock (HF) equations. At the level of the HF equation the original N-body problem has already been reduced to a system of N coupled stationary "one-electron" Schrödinger equations. The derivation of the stationary HF equation is essentially based on a minimization of the total energy of the N-body Schrödinger equation for antisymmetric wave functions, taken as "Slater-determinants" :

$$\Psi(\mathbf{x}_1, \cdots, \mathbf{x}_N) = \frac{1}{\sqrt{N!}} \det\left(\psi_k(\mathbf{x}_j)\right)_{j,k=1,\cdots,N} . \tag{1.3}$$

The stationary HF equations for the set of N orthonormal "one particle" wavefunctions ψ_j are

$$-\frac{\varepsilon^2}{2}\Delta\psi_j + V_{\text{ext}}\,\psi_j + V_{\text{Hartree}}\,\psi_j + (V_{\text{exc}}\psi)_j \;=\; E_j\,\psi_j \;; \quad j = 1, \cdots, N, \tag{1.4}$$

where E_j is the j-th eigenvalue, V_{ext} stands for a given external potential, V_{Hartree} is the Hartree potential, with the local density ρ:

$$V_{\text{Hartree}}(\mathbf{x}) := \int_{I\!R^d} \frac{\rho(\mathbf{y})}{|\mathbf{x}-\mathbf{y}|} d\mathbf{y}, \qquad \rho(\mathbf{x}) := \sum_{j=1}^{N} |\psi_j(\mathbf{x})|^2, \qquad \mathbf{x} \in I\!R^d \tag{1.5}$$

and $(V_{\text{exc}}\psi)_j$ is the exchange-term, defined by

$$(V_{\text{exc}}\psi)_j(\mathbf{x}) := -\sum_{k=1}^{N} \left\{ \int_{I\!R^d} d\mathbf{x}' \frac{\psi_j(\mathbf{x}')\overline{\psi_k}(\mathbf{x}')}{|\mathbf{x}-\mathbf{x}'|} \right\} \psi_k(\mathbf{x}) , \qquad 1 \le j \le N . \tag{1.6}$$

For a rigorous analysis of this stationary Hartree-Fock system and references see e.g. [Lio1]. For the time-dependent case, the rigorous derivation of the HF equations formulated for the density matrix, by means of "mean field limits", is given in [BM2] for bounded interactions and in [BM3] for the Coulomb case which we are dealing with in the present paper.

Note that the HF exchange potential (1.6) not only couples the N equations for the N one-particle wave functions ψ_j, but is different for each of the equations and nonlocal in position $\mathbf{x}$. For a large number N of electrons, the HF model becomes too complex for practical calculations and it is necessary to replace the HF system by simpler equations, in particular when we leave the regime of atoms and regard electrons in a semiconductor, where N is of order 10^3 up to 10^{26}.

Unlike the atomic case, in this situation also a solution of the Kohn-Sham equations (i.e. the N coupled equations (1.4) with the nonlocal exchange term (1.6) replaced by the local $X\alpha$ term defined below) is out of question and only some sort of "single particle" ("mean field") equation can be handled.

An astonishingly simple approximation of the exchange potential in (1.4) or (1.6) is due to Slater [Sla] who replaces the term $(V_{\text{exc}}\psi)_j$ by

$$(V_{\text{exc}}\psi)_j(\mathbf{x}) \simeq V_S(\mathbf{x})\psi_j(\mathbf{x}) := -C\rho^{1/3}(\mathbf{x})\;\psi_j(\mathbf{x}) , \qquad \mathbf{x} \in I\!R^d, \quad 1 \le j \le N, \tag{1.7}$$

where $C > 0$ is a constant. The local expression (1.7) was first given implicitly by Dirac [D1] in the context of the exchange energy as a correction in the Thomas-Fermi

model. It is also named after Gaspar [G1] and Kohn-Sham [KS] where it appears with a difference of 2/3 in the factor C in (1.7). By the name "$X\alpha$ method" [PY, Co], these expressions are summarized in the sense that the value of this constant is named α and taken as parameter tunable in a certain range.

The key assumption for using the approximation (1.7) is that the density $\rho(\mathbf{x})$ is "close" to the constant density of plane waves ("free electron") [Sla]. This term (1.7) has the additional advantage that it models the exchange interaction without wave functions and can hence be used also in "classical" models invoking Fermi-Dirac statistics where an exchange term should be included for reasons of consistency [M1].

Despite the successful use of this kind of local approximations of the HF exchange potential, rigorous derivations are still missing. In a particular setting on the torus a rigorous version of Slater's heuristic arguments to derive the $X\alpha$ exchange potential was given in [BM1],[BGM], and in [Ba1] a more general derivation for the local approximation of the "Dirac-term" [D1] in the exchange energy was given.

For the time-dependent case the problem of rigorously deriving time-dependent nonlinear one particle Schrödinger equations as approximations of the linear N particle Schrödinger equation (1.1) is mostly open, with the derivation of the Schrödinger-Poisson equation based on a Hartree ansatz for Ψ_I as the only case solved so far [BMY].

In this paper, we study the S-P-Xα model with/without an external potential numerically in order to understand effective one particle quantum dynamics of electrons and get insight into the semi-classical limit of the S-P-Xα model.

This paper is organized as follows: In section 2, we present and heuristically motivate the S-P-Xα model, review its existence and uniqueness results and present the Wigner-Poisson-Xα (W-P-Xα) model. In section 3, we present the time-splitting spectral method for numerical solution of the S-P-Xα model, its implementation on a parallel computer as well as how to compute the Wigner measures numerically from the wave function. In section 4, we present numerical results of position density and Wigner measures in 1d, 2d and 3d for the S-P-Xα model with/without an external potential. In section 5, we draw some conclusions.

2. The Schrödinger-Poisson-Xα equation

In order to take into account exchange effects in a time-dependent one-particle approximation, we can most simply take the more or less rigorously derived expression of the stationary case and hence add the "$X\alpha$" term (1.7), with t as additional variable, to the effective potential in the Schrödinger-Poisson model. This corresponds to "time dependent density functional theory", where the energy is expressed in terms of the local density $\rho(x,t)$. This yields a NLS with a "weak" nonlocal nonlinearity, and a "strong" local nonlinearity with a potential that is a power of the local density.

In a model with d space dimensions, the approximated exchange term (1.7) is proportional to $\rho^{1/d}$, according to the derivation in [BM1]. In 1d, i.e. $d = 1$ in (2.1), the $X\alpha$ term is exactly what is called the "focusing cubic NLS", i.e. $-\alpha\,|\psi|^2\psi$.

We call the equations (2.1), (2.2) the "Schrödinger-Poisson-$X\alpha$" (S-P-Xα) model:

$$i\varepsilon\partial_t\psi = -\frac{\varepsilon^2}{2}\Delta\psi \;+\; C\,V_{\rm Hartree}\;\psi \;-\; \alpha\,|\psi|^{2/d}\psi \;+\; V_{\rm ext}\psi, \quad \mathbf{x}\in I\!R^d,\ t\in I\!R\,, \tag{2.1}$$

$$\Delta V_{\rm Hartree} = -|\psi|^2, \tag{2.2}$$

$$\psi(\mathbf{x}, t=0) = \psi_I(\mathbf{x}), \qquad \mathbf{x}\in I\!R^d\,; \tag{2.3}$$

where $C > 0$ is a fixed constant, $\alpha > 0$ a parameter and $V_{\rm ext}$ is a given external potential, for example a confining potential.

Since $C > 0$ and $\alpha > 0$, we have a repulsive Hartree interaction and a focusing local nonlinearity. The wave function ψ is used to compute the physical observables, e.g. the position density

$$n(\mathbf{x}, t) = |\psi(\mathbf{x}, t)|^2, \qquad \mathbf{x} \in I\!R^d, \quad t \geq 0. \tag{2.4}$$

Note that the inclusion of the $X\alpha$ term for the time-dependent case lacks a rigorous justification. However, it seems more reasonable to include this term, which is justified in the stationary case, than to totally neglect the Pauli principle and use the S-P model, as it is mostly done. The underlying physical interpretation via the "exchange-correlation hole" makes sense also in the time-dependent case.

2.1. Existence and uniqueness of solutions. At ε fixed, the analysis of equation (2.1)-(2.3) in 3-d can be done by a straightforward application of standard results on NLS [B], [Caz], [GV], [KPV]. We use a result from [Caz]. We first formulate a slightly more general form of the equation, with ε set to 1:

$$i\partial_t \psi = -\Delta\psi \; - \; C\,(g(\mathbf{x}) * |\psi|^2)\psi \; - \; \lambda\,|\psi|^p\psi, \qquad \mathbf{x} \in I\!R^d, \quad t \in I\!R\,, \tag{2.5}$$

$$\psi(\mathbf{x}, t = 0) = \psi_I(\mathbf{x}), \qquad \mathbf{x} \in I\!R^d\,; \tag{2.6}$$

where C, λ are real parameters and $g(\mathbf{x})$ is a given real-valued potential. So in this model, a defocusing ($\lambda < 0$)/ focusing ($\lambda > 0$) local nonlinearity and a nonlocal Hartree interaction are included.

For the general NLS (2.5), Cazenave ([Caz], Thm. 6.1.1, Ex. 1) proved the following results of global existence in the "energy space" H^1: Let $g(\mathbf{x})$ be an even, real-valued potential belonging to $L^\sigma(I\!R^d) + L^\infty(I\!R^d)$, for some $\sigma \geq 1$, $\sigma > \frac{d}{4}$. Let either $\lambda \leq 0$ and $p < \frac{4}{d-2}$($p < \infty$ if $d = 1$ or $d = 2$, defocusing case) or $\lambda > 0$ and $p < \frac{4}{d}$ (focusing case). Let $\psi_I \in H^1(I\!R^d)$. Then equation (2.5) has a unique global solution $\psi \in C(I\!R, H^1(I\!R^d)) \cap C^1(I\!R, H^{-1}(I\!R^d))$.

So our exponent $2/d$ in (2.1) is sub-critical in the defocusing as well as in the focusing case. The assumptions on $g(\mathbf{x})$ are satisfied by the Green function of the Hartree potential in 3 dimensions.

In fact, Cazenave ([Caz], Thm. 6.3.2, Rem. 6.3.4) also proved existence results in L^2 for (2.5): Let $g(\mathbf{x})$ be an even, real-valued potential belonging to $L^\sigma(I\!R^d) + L^\infty(I\!R^d)$, for some $\sigma \geq 1$, $\sigma > \frac{d}{2}$ ($\sigma > 1$ if $d = 2$). Let $p < \frac{4}{d}$, $r = p + 2$, and let q be defined by

$$\frac{2}{q} = d\left(\frac{1}{2} - \frac{1}{r}\right). \tag{2.7}$$

Then, for every $\psi_I \in L^2(I\!R^d)$ there exists a unique $\psi \in C(I\!R, L^2(I\!R^d)) \cap L^q_{loc}(I\!R, L^r(I\!R^d))$ with $\psi_t \in L^q_{loc}(I\!R, H^{-2}(I\!R^d))$, solution of (2.5). In addition, we have $\|\psi(t)\|_{L^2} = \|\psi_I\|_{L^2}$ for all $t \in I\!R$, and ψ in $L^{q'}_{loc}(I\!R, L^{r'}(I\!R^d))$ for every index pair (q', r') with $r' \in [2, \frac{2d}{d-2})$ and q' defined by (2.7). Furthermore, if $\phi_m \to \phi$ in $L^2(I\!R^d)$ and if ψ_m denotes the solution of (2.5) with initial datum ϕ_m, then $\psi_m \to \psi$ in $L^{q'}_{loc}(I\!R, L^{r'}(I\!R^d))$, for every index pair (q', r') as defined above.

For the 1-d case, the existence and uniqueness analysis of the S-P-Xα equation is given in [Stim1], following the approach of Steinrück for the 1-d Schrödinger-Poisson equation [Ste1]. For the case of 2 space dimensions, the analysis of the S-P-Xα equation is open.

2.2. Wigner-Poisson-Xα model. The limit of $\varepsilon \to 0$, the so-called "semi-classical limit", is a mostly open problem for (2.1)-(2.3). The Wigner transform [LP], [GMM] is a perfect tool for performing certain classes of (semi)classical limits, in particular from the weakly nonlinear Schrödinger-Poisson system, i.e. (2.1) - (2.2) with $\alpha = 0$, to the Vlasov-Poisson system via the Wigner-Poisson system (2.9) - (2.12) (cf [MM1], [LP]). The Wigner transform $w^\varepsilon[\psi](\mathbf{x},\xi)$ of $\psi(\mathbf{x}) \in L^2$ is defined as the "phase-space" function

$$w^\varepsilon[\psi](\mathbf{x},\xi) = (2\pi)^{-d} \int_{I\!R^d_\eta} \psi\left(\mathbf{x} - \varepsilon\frac{\eta}{2}\right) \overline{\psi}\left(\mathbf{x} + \varepsilon\frac{\eta}{2}\right) e^{i\eta\cdot\xi} d\eta\,. \tag{2.8}$$

Taking the Wigner transform of (2.1), we obtain the "Wigner-Poisson-Xα" (W-P-Xα) model:

$$\frac{\partial}{\partial t} w^\varepsilon + \xi\cdot\nabla_{\mathbf{x}} w^\varepsilon + \Theta[V_{\rm Hartree}] w^\varepsilon - \alpha\,\Theta[\rho^{1/d}] w^\varepsilon \;+\; \Theta[V_{\rm ext}] w^\varepsilon = 0, \quad \mathbf{x}\in I\!R^d,\ \xi\in I\!R,\ t>0, \tag{2.9}$$

where $w^\varepsilon(\mathbf{x},\xi,t)$ is the real-valued Wigner transform of $\psi(\mathbf{x},t)$ and $\Theta[.]$ are the pseudo–differential operators corresponding to the potentials as the following "Fourier multiplier"

$$\Theta[V](\mathbf{x},\xi,t) = \frac{i}{(2\pi)^m} \int_{I\!R_\eta} \frac{V(\mathbf{x}+\frac{\varepsilon}{2}\eta,t) - V(\mathbf{x}-\frac{\varepsilon}{2}\eta,t)}{\varepsilon} \hat{w}(\mathbf{x},\eta,t) e^{i\xi\cdot\eta} d\eta, \tag{2.10}$$

where " $\hat{}$ " stands for the Fourier transform with respect to the velocity variable ξ. The physical quantities are now calculated as moments of the (not strictly positive !) Wigner function. The position (charge) density reads

$$\rho(\mathbf{x},t) \;=\; \int_{I\!R_\xi} w^\varepsilon(\mathbf{x},\xi,t) d\xi, \qquad \mathbf{x}\in I\!R^d, \quad t>0 \tag{2.11}$$

and the coupling to the Poisson equation reads:

$$\Delta V_{\rm Hartree}(\mathbf{x},t) \quad = \quad -\,\rho(\mathbf{x},t), \qquad \mathbf{x}\in I\!R^d, \quad t>0. \tag{2.12}$$

The use of Wigner functions as a phase space representation of quantum mechanics is also common in applications like "quantum state tomography" [SSJM].

For calculating the semi-classical limit, the following property of the Wigner transform is crucial. For a sequence ψ^ε uniformly bounded in L^2 we have:

$$w^\varepsilon[\psi^\varepsilon](\mathbf{x},\xi) \overset{\varepsilon\to 0}{\rightharpoonup} w^0[\psi^\varepsilon](\mathbf{x},\xi), \qquad \text{in } \mathcal{D}', \tag{2.13}$$

where $w^0(\mathbf{x},\xi)$ is a non-negative measure on the phase space: the "semi-classical" or "Wigner measure" of the sequence ψ^ε (which is not necessarily unique).

However, the local $(X\alpha)$ term in our NLS does not allow a straightforward application of Wigner transform techniques, as they have been successfully used for the Schrödinger-Poisson equation - see [M3] for an overview of recent results. The formal (!) limit of the W-P-Xα equation is given by the nonlinear Vlasov equation for the nonnegative weak limit $w^0(\mathbf{x},\xi,t) \ge 0$ of $w^\varepsilon(\mathbf{x},\xi,t)$

$$\partial_t w^0 + \xi\cdot\nabla_{\mathbf{x}} w^0 - \nabla_{\mathbf{x}} V_{\rm Hartree}\cdot\nabla_\xi w^0 \;-\; \nabla_{\mathbf{x}} V_{\rm ext}\cdot\nabla_\xi w^0 = \alpha\,\nabla_{\mathbf{x}}(\rho^{1/3})\cdot\nabla_\xi w^0, \tag{2.14}$$

with $\rho(\mathbf{x},t) = \int_{\mathbb{R}_\xi} w^0(\mathbf{x},\xi,t)d\xi$. This limit does not make sense at discontinuities of $\rho(\mathbf{x},t)$ (in $\mathbf{x}$), the right hand side of (2.14) would mean a multiplication of a δ-measure with a function which is discontinuous at the point of concentration of the δ-measure, which does not have a meaning (cp. however the concept of measure valued (non-unique !) solutions of Vlasov-Poisson as used in [ZZM], using Volpert's symmetric average). In [Car] the semi-classical limit $\varepsilon \to 0$ is obtained in the case of a particular geometry where geometric arguments can be applied, and scattering operators are used at the discontinuity points of $\rho(\mathbf{x},t)$. The general problem of the semi-classical limit of the NLS (2.1) still remains open.

Note that Wigner measures are also an appropriate tool to study numerical methods for NLS [MPP], [MPPS].

We will report Wigner transforms for decreasing ε for some of our numerical results in the next chapter, which were calculated from the wave function at fixed time. Some information on the limiting Wigner measure can be obtained from such "numerical semi-classics".

3. Numerical method and implementation for the S-P-Xα model

3.1. Time-splitting spectral scheme. In order to solve (2.1) numerically, we adapt the time-splitting spectral code of [BJM1] ("Fourier split-step method" [WH]). This method was recently used and studied for NLS in the semi-classical regime [BJM2] and showed much better spatial and temporal resolution than the finite difference method [MPP], [MPPS]. It is hence also the method of choice to discretize the S-P-Xα model.

We impose periodic boundary conditions for convenience to use the spectral method. By choosing a sufficiently large domain of computation we can avoid spurious effects for the time regime we regard.

The merit of this numerical method for NLS is that it is explicit, unconditionally stable, time reversible, time-transverse invariant and it conserves the position density [BJM1]. Also it has very favorable properties with respect to efficiently choosing the spatial/temporal grid in dependence of the semi-classical parameter ε [BJM1]. For simplicity of notation we shall introduce the method in one space dimension ($d = 1$). Generalizations to $d > 1$ are immediate for tensor product grids and the results remain valid without modifications.

For $d = 1$, eqs. (2.1)-(2.3) with periodic boundary conditions become:

$$i\varepsilon\partial_t\psi = -\frac{\varepsilon^2}{2}\partial_{xx}\psi + C\,V_{\text{Hartree}}\,\psi - \alpha\,|\psi|^{2/d}\psi + V_{\text{ext}}\psi,\ a\le x\le b,\ t>0\,, \quad (3.1)$$

$$\partial_{xx}V_{\text{Hartree}} = -|\psi|^2, \qquad a \le x \le b, \quad t > 0, \quad (3.2)$$

$$\psi(a,t) = \psi(b,t),\ \psi_x(a,t) = \psi_x(b,t),\ V_{\text{Hartree}}(a,t) = V_{\text{Hartree}}(b,t) = 0,\ t\ge 0, \quad (3.3)$$

$$\psi(x,t=0) = \psi_I(x),\ a \le x \le b. \quad (3.4)$$

We choose the spatial mesh size $h = \Delta x = (b-a)/M > 0$ with M an even positive integer, the time step $k = \Delta t > 0$, and denote $x_j = a + jh$ ($j = 0,\ldots,M$), $t_n = nk$ ($n = 0,1,\ldots$) the grid points. Let ψ_j^n be the approximation of $\psi(x_j,t_n)$ and ψ^n be the solution vector with components ψ_j^n.

The idea behind the time splitting spectral method for the S-P-Xα model is to decouple the nonlinear partial differential equations into a linear PDE with constant coefficients, which can be discretized in space by the spectral method and integrated in time **exactly**, and a nonlinear ordinary differential equation which can also be

solved **exactly**. From time $t = t_n$ to $t = t_{n+1}$, the S-P-Xα equation is solved in two splitting steps. One solves first

$$i\varepsilon\partial_t\psi = -\frac{\varepsilon^2}{2}\Delta\psi, \qquad a \le x \le b, \tag{3.5}$$

for the time step of length k, followed by solving

$$\partial_{xx} V_{\text{Hartree}} = -|\psi|^2, \tag{3.6}$$

$$i\varepsilon\partial_t\psi = C\, V_{\text{Hartree}}\ \psi - \alpha\ |\psi|^{2/d}\psi + V_{\text{ext}}\ \psi, \qquad a \le x \le b, \tag{3.7}$$

for the same time step. Eq. (3.5) will be discretized in space by the Fourier spectral method due to the periodic boundary conditions (3.3) and integrated in time **exactly**. For $t \in [t_n, t_{n+1}]$, the ODE (3.7) leaves $|\psi|$ invariant in t [BJM1] and therefore becomes

$$\partial_{xx} V_{\text{Hartree}} = -|\psi(x,t_n)|^2, \tag{3.8}$$

$$i\varepsilon\partial_t\psi(x,t) = C\, V_{\text{Hartree}}\ \psi(x,t) - \alpha\ |\psi(x,t_n)|^{2/d}\psi(x,t) + V_{\text{ext}}\ \psi(x,t), a \le x \le b. \tag{3.9}$$

Thus eq. (3.8) will be discretized by the Fourier spectral method when $|\psi|$ is given and (3.9) can be integrated **exactly**. From time $t = t_n$ to $t = t_{n+1}$, we combine the splitting via the standard second-order splitting:

$$\psi_j^* = \frac{1}{M}\sum_{l=-M/2}^{M/2-1} e^{-i\varepsilon\mu_l^2\, k/4}\ \widehat{(\psi^n)}_l\ e^{i\mu_l(x_j-a)}, \quad j = 0,1,2,\cdots,M-1,$$

$$(V_{\text{Hartree}})_j^* = \frac{1}{M}\sum_{-M/2\le l\le M/2-1,\ l\ne 0} \widehat{(|\psi^*|^2)}_l/\mu_l^2\ \ e^{i\mu_l(x_j-a)}, \quad j = 0,1,2,\cdots,M-1,$$

$$\psi_j^{**} = e^{-i[C\,(V_{\text{Hartree}})_j^* + V_{\text{ext}}(x_j) - \alpha|\psi_j^*|^{2/d}]k/\varepsilon}\ \psi_j^*, \qquad j = 0,1,2,\cdots,M-1,$$

$$\psi_j^{n+1} = \frac{1}{M}\sum_{l=-M/2}^{M/2-1} e^{-i\varepsilon\mu_l^2\, k/4}\ \widehat{(\psi^{**})}_l\ e^{i\mu_l(x_j-a)}, \quad j = 0,1,2,\cdots,M-1; \tag{3.10}$$

where $\widehat{U}_l$ ($l = -M/2,\cdots,M/2-1$), the Fourier coefficients of a vector $U = (U_0, U_1, \cdots, U_M)^T$ with $U_0 = U_M$, are defined as

$$\mu_l = \frac{2\pi l}{b-a}, \qquad \widehat{U}_l = \sum_{j=0}^{M-1} U_j\ e^{-i\mu_l(x_j-a)}, \quad l = -\frac{M}{2},\cdots,\frac{M}{2}-1. \tag{3.11}$$

The Wigner transform $W[\psi](x,\xi)$ of a given discretized wave function is then calculated by using formula (2.8) and a standard numerical integration procedure.

3.2. Realization on a parallel machine. For simulations in 3 space dimensions with a satisfactory space resolution a large amount of memory is needed, exceeding the limitations of standard single processor computers. For such simulations parallel computers are very appropriate. This requires of course an adaptation of the code which can not be done automatically.

We are using the cluster "Schrödinger 2" of the University of Vienna, which currently features 192 Pentium IV processors, with about 1 GB memory each, linked by a switched gigabit network. The machine's LINPACK performance ranges among the fastest available.

TABLE 3.1. *Memory requirement for 3-d calculation*

Resolution	Memory requirement
256 points per dimension	$8 \cdot 10^8$ byte = 768 MB
512 points per dimension	$6.4 \cdot 10^9$ byte = 6.4 GB
1024 points per dimension	$5.1 \cdot 10^{10}$ byte = 48 GB
16 byte numbers (type 'double complex'), 3 instances needed	

As the above table shows, 64 nodes of this parallel machine are sufficient for 3-d simulations with a resolution with about 1000 points in each space dimension.

We use the MPI parallelization interface to adapt the code for distributed memory parallelization and compile it with "ifc", a Fortran compiler made by Intel. Hence both the compiler and the processor hardware come from the same manufacturer, which made it relatively easy to generate code optimized specifically for the used processor type and to obtain a quite good performance.

The main workload of the scheme, and the only part of the actual algorithm which needs to be adapted for parallelization, consists of Fast Fourier transforms. We implement a parallel version of an FFT code on the cluster "Schrödinger 2" and test the performance of the parallelization which is listed in Table 2.

We see from table 2 that the code has a good degree of parallelization in the sense that most of the work seems to be evenly distributed among the nodes and calculation time decreases linearly with the number of nodes used. (The final version of the machine is actually faster than in table 2, reducing the required CPU time once more.)

TABLE 3.2. *Performance*

	256^3 grid points, walltime	
Number of nodes	50 time steps	500 time steps
2	1527 s	14760 s
4	812 s	7860 s
8	432 s	4020 s

In all our 3d simulations, we use the parallel code of the time-splitting spectral method (TSSP) to compute our numerical results.

4. Numerical results

In this section, we will present 1-d, 2-d and 3-d numerical results of the S-P-Xα model by using the time-splitting spectral discretization.

In our computations, the initial condition for (2.1)-(2.3) is always chosen in the WKB form:

$$\psi(\mathbf{x}, t=0) = \psi_I(\mathbf{x}) = A_I(\mathbf{x}) e^{i\, S_I(\mathbf{x})/\varepsilon}, \qquad \mathbf{x} \in I\!R^d, \tag{4.1}$$

with A_I and S_I real valued, regular and with A_I decaying to zero sufficiently fast as $|\mathbf{x}| \to \infty$. We always compute on a domain which is large enough (as controlled by the initial data and how long in time to compute) such that the periodic boundary

conditions do not introduce a significant aliasing error relative to the whole space problem. To visualize our numerical results, we always present the position density $n(\mathbf{x}, t)$ which is defined as

$$n(\mathbf{x}, t) = |\psi(\mathbf{x}, t)|^2, \qquad \mathbf{x} \in I\!R^d.$$

Example 1. 1-d S-P-Xα model, i.e. we choose $d = 1$, $V_{\text{ext}} \equiv 0$, $C = 1$ in (2.1). Note that the local interaction term in (2.1) is the "focusing cubic NLS interaction" in the case $d = 1$. The initial condition (4.1) is hence taken the same as in the simulations of [MK]:

$$A_I = e^{-x^2}, \qquad \frac{d}{dx} S_I(x) = -\tanh(x), \qquad -\infty < x < \infty. \tag{4.2}$$

Note that S_I is such that the initial phase is compressive. This means that even the linear evolution develops caustics in finite time. We solve this problem either on the interval $x \in [-4, 4]$ or on $x \in [-8, 8]$ depending on the time for which the solution is calculated.

We present numerical results for four different regimes of α:

Case I. $\alpha = 0$, i.e Schrödinger-Poisson regime;
Case II. $\alpha = \varepsilon$, i.e. Schrödinger-Poisson equation with $O(\varepsilon)$ cubic nonlinearity;
Case III. $\alpha = \sqrt{\varepsilon}$, i.e. Schrödinger-Poisson equation with $O(\sqrt{\varepsilon})$ cubic nonlinearity;
Case IV. $\alpha = 1$, i.e. Schrödinger-Poisson equation with $O(1)$ cubic nonlinearity.

Figure 4.1 displays comparisons of the position density $n(x, t)$ at fixed time for the above four different parameter regimes with different ε. Figure 4.2 plots the evolution of the position density and the Wigner transforms of the wave function for $\alpha = 1$ and $\varepsilon = 0.025$. Figure 3 shows the analogous results for attractive Hartree interaction, i.e. $C = -1$, $\alpha = 0.5$ and $\varepsilon = 0.025$.

From Figure 4.1, we can see that before the "break time"("caustic"), the result is essentially independent of ε. After the break the behavior of the position density changes substantially with respect to the different regimes of α. For $\alpha = 0$ the solution stays smooth. For $\alpha = \varepsilon$ it stays also smooth, but it concentrates at the origin. For $\alpha = \sqrt{\varepsilon}$ a pronounced structure of peaks develop, that look like the soliton structure typical for the NLS [MK]. The number of peaks is doubled when ε is halved. For $\alpha = 1$, the number of peaks increases again and they occur at different locations than for $\alpha = \sqrt{\varepsilon}$.
We can see that the scaling $\alpha = \mathrm{O}(\sqrt{\varepsilon})$ is critical in the sense that the solution has a substantially different behavior than for the smaller scales of α. Beyond this scaling, the semiclassical limit cannot be obtained by naive numerics.

Figure 4.2 b) shows how the Wigner function completely changes its qualitative behaviour after the "break time" ("caustic") and develops a rich structure of oscillations.

Figure 4.3 is a test to see what happens if the Hartree potential is attractive instead of repulsive, with all other parameters kept the same, i.e. Figure 4.2 a) and Figure 4.3 differ only by the sign of C. The resulting effect corresponds to the physical intuition that the pattern of caustics that is typical for the focusing NLS would be enhanced and focused in physical space by an additional attractive force.

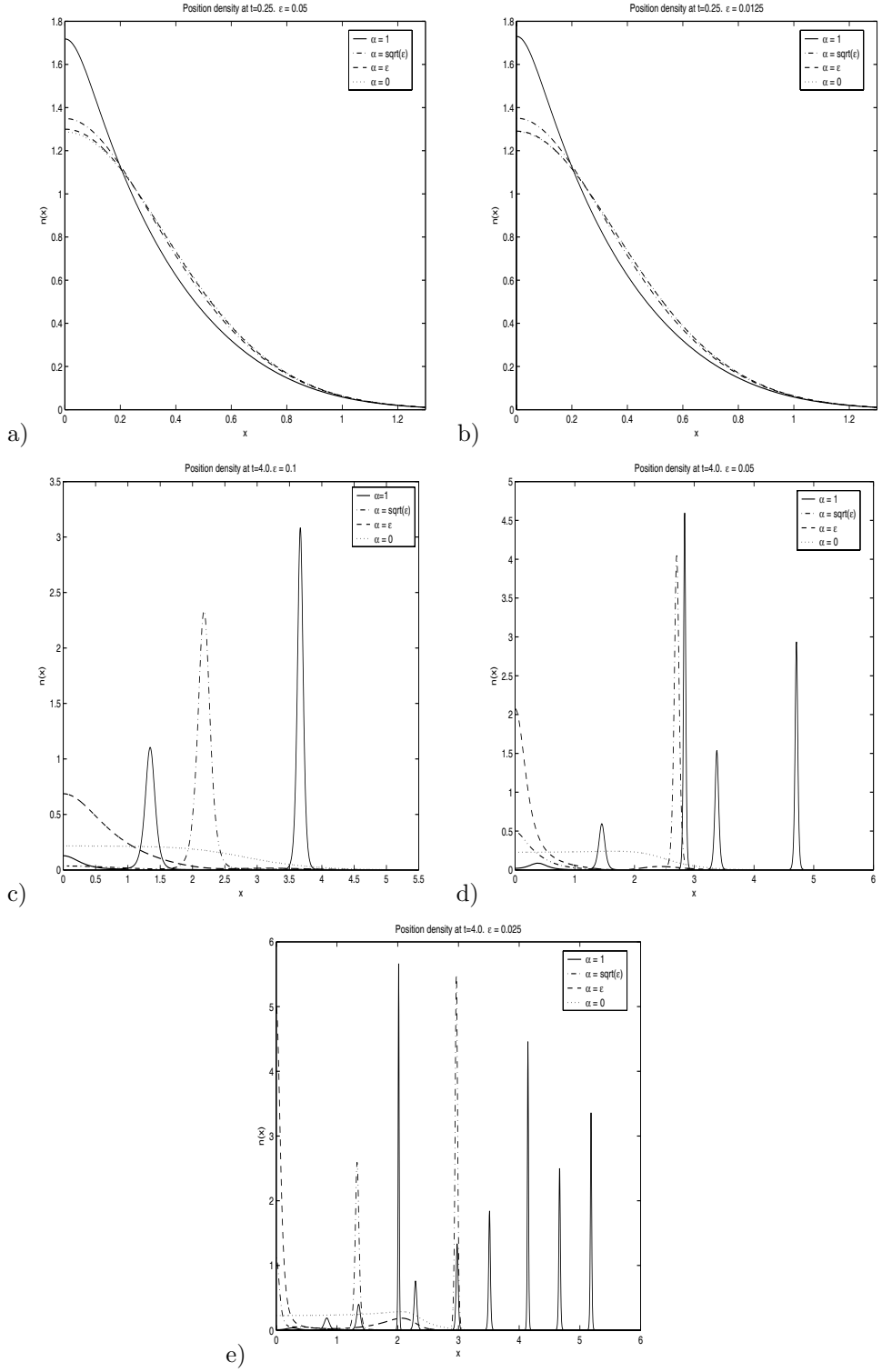

FIG. 4.1. *Numerical results for different scales of the Xα term, i.e.* $\alpha = 1,\ \sqrt{\varepsilon},\ \varepsilon,\ 0$. *a) - b): small time* $t = 0.25$, *pre-break, a) for* $\varepsilon = 0.05$, *b) for* $\varepsilon = 0.0125$. *c) - e): large time,* $t = 4.0$, *post-break. c) for* $\varepsilon = 0.1$, *d) for* $\varepsilon = 0.05$, *e) for* $\varepsilon = 0.025$.

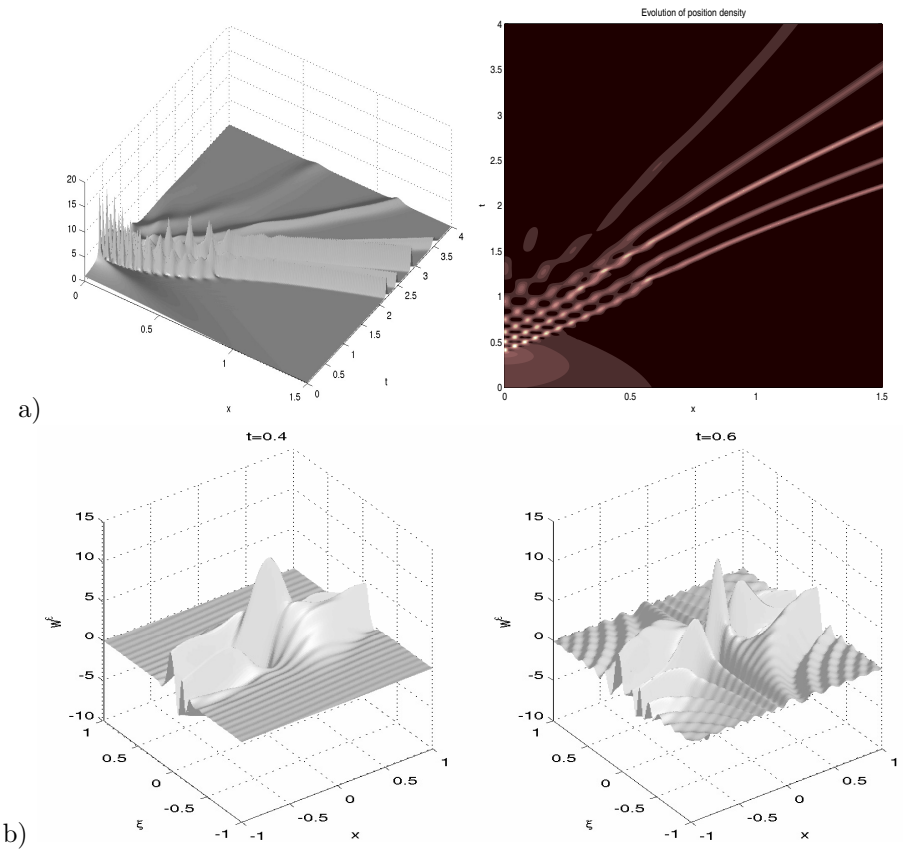

FIG. 4.2. *Numerical results for Xα term at O(1), i.e. α = 0.5, with ε = 0.025, h = 1/512 and k = 0.0005. a) Time evolution of the position density n(x,t) = |ψ(x,t)|²: Left: surface plot; Right: pseudocolor plot. b) Wigner function W[ψ(x,t)] at different times.*

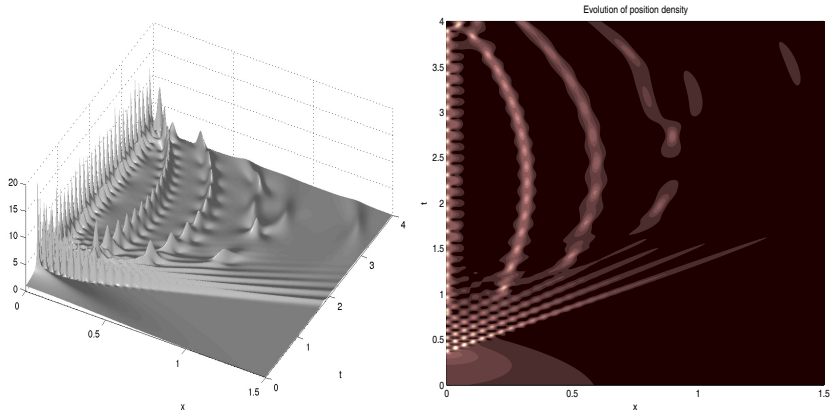

FIG. 4.3. *Time evolution of the position density for attractive Hartree interaction, i.e. C = −1, α = 0.5, ε = 0.025, Δt = 0.00015. Left: surface plot; right: pseudocolor plot.*

Example 2. 2-d S-P-Xα model, i.e. we choose $d = 2$ in (2.1). Three types of initial data (4.1) are considered:
Data 1. Symmetric initial data with zero phase:

$$A_I(x,y) = e^{-(x^2+y^2)}, \qquad S_I(x,y) = 0; \tag{4.3}$$

Data 2. Symmetric initial data with nonzero phase:

$$A_I(x,y) = e^{-(x^2+y^2)}, \qquad S_I(x,y) = \ln\cosh\left(\sqrt{x^2+y^2}\right); \tag{4.4}$$

Data 3. Non-symmetric initial data with zero phase:

$$A_I(x,y) = e^{-(x^2+y^2)} - 0.2e^{-(25x^2+y^2)}; \tag{4.5}$$

The domain of computation is the rectangle $[-4,4]^2$.
Figure 4.4 shows the position density $n(x,y,t)$ for the above three different initial data with $\alpha = 1$, $C = 1$, $\varepsilon = 0.04$ and $V_{\text{ext}} \equiv 0$. Figure 4.5 displays the Wigner functions for data 1 and $\alpha = 1$, $C = 1$, $V_{\text{ext}} \equiv 0$. Furthermore Figure 4.6 shows the evolution of the position density of slice $y = 0$, i.e. $n(x,0,t)$ with data 3, $\alpha = 0.5$, $C = 0$, and a nonzero external potential $V_{\text{ext}} = \frac{\omega^2}{2}(x^2+y^2)$, $\varepsilon = 0.04$ for 2 different values of the "confining frequency" ω.

In Figure 4.4, we illustrate how the choice of the phase influences the pattern formation in time for identical initial amplitude, but that a nonsymmetric amplitude creates complex peak patterns also for a zero initial phase.

The first 3 Wigner measures of Figure 4.5 correspond to 3 different values of ε, indicating the form of the semiclassical measure, as far as a function in 4 variables can be presented.

The simulation of Figure 4.6, for the initial data with non-zero phase, show the effect of a quadratic confinement potential which corresponds to a harmonic oscillator. By doubling the frequency ω from Fig. a) to b) we observe twice as many "oscillations" of the pattern.

Example 3. 3-d S-P-Xα model, i.e. we choose $d = 3$, $V_{\text{ext}} \equiv 0$, $C = 1$ in (2.1). We consider two types of initial data.

Data 1. Symmetric initial data with nonzero phase:

$$A_I(x,y,z)=e^{-(x^2+y^2+z^2)}, \quad S_I(x,y,z)=-\ln\cosh\left(\sqrt{x^2+y^2+z^2}\right); \tag{4.6}$$

Data 2. Non-symmetric initial data with zero phase:

$$A_I(x,y,z) = e^{-(x^2+y^2+z^2)} - 0.2e^{-(25x^2+y^2+z^2)}; \tag{4.7}$$

We solve this problem on the box $[-8,8]^3$. For data 1, we will present numerical results for five different regimes of α:

Case I. $\alpha = 0$, i.e Schrödinger-Poisson regime;
Case II. $\alpha = \varepsilon^2$, i.e. Schrödinger-Poisson equation with Xα nonlinearity at $O(\varepsilon^2)$;
Case III. $\alpha = \varepsilon$, i.e. Schrödinger-Poisson equation with Xα nonlinearity at $O(\varepsilon)$;
Case IV. $\alpha = \sqrt{\varepsilon}$, i.e. Schrödinger-Poisson equation with Xα nonlinearity at $O\left(\sqrt{\varepsilon}\right)$;
Case V. $\alpha = 1$, i.e. Schrödinger-Poisson equation with Xα nonlinearity at $O(1)$.

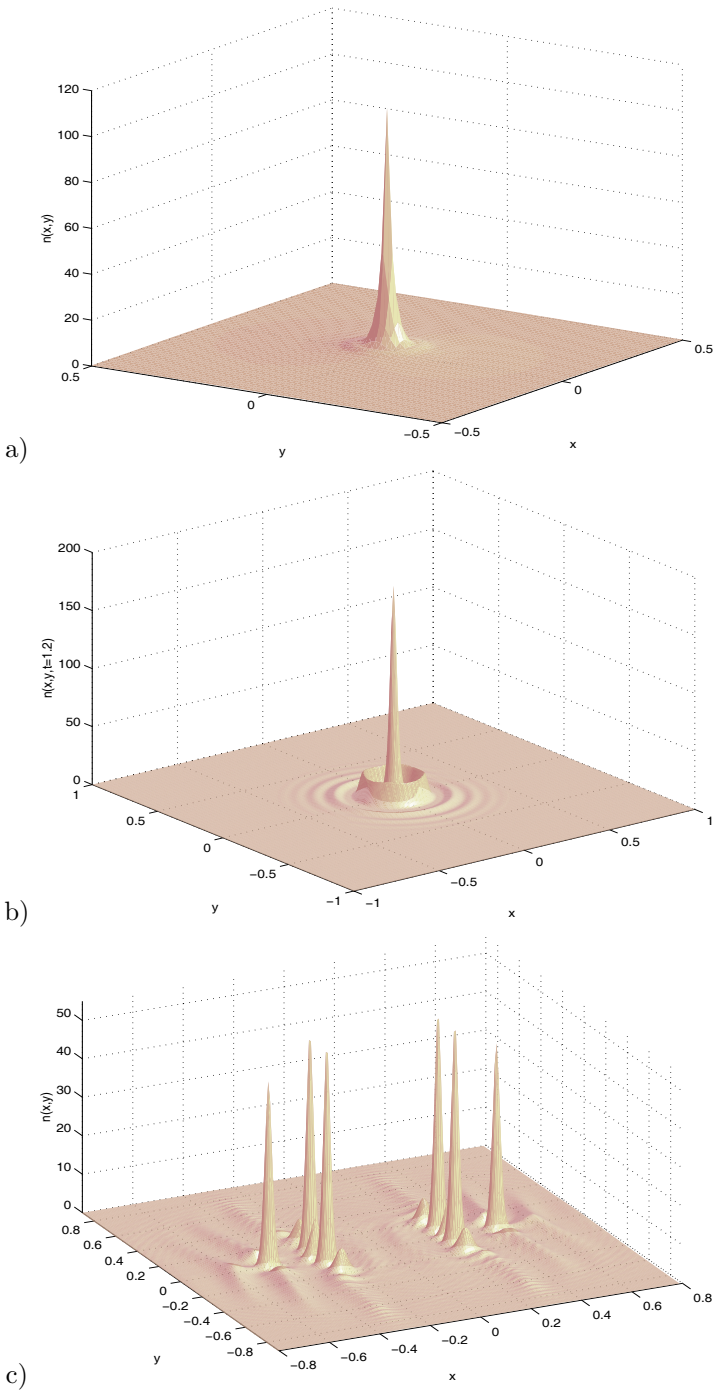

FIG. 4.4. *Position density* $n(x, y, t)$ *for different initial data with* $\alpha = 1$, $C = 1$, $\varepsilon = 0.04$ *and* $V_{\text{ext}} \equiv 0$ *in example 2. a) At* $t = 0.75$ *for data 1; b) At* $t = 1.2$ *for data 2; c) At* $t = 0.8$ *for data 3.*

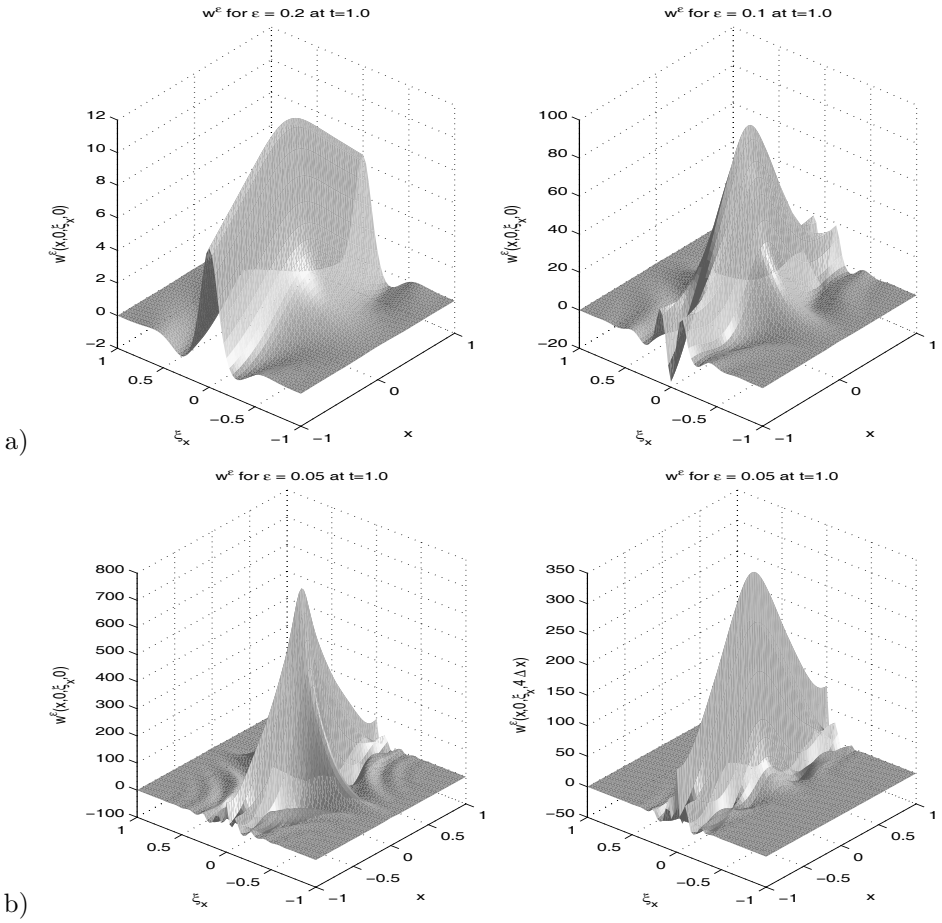

FIG. 4.5. *"Numerical semiclassics" ($\varepsilon = 0.2, 0.1, 0.05$) for the Wigner function in example 2 with initial data case 1 and $\alpha = 1$, $C = 1$, $V_{\text{ext}} \equiv 0$. a) Left: $\varepsilon = 0.2$, Right: $\varepsilon = 0.1$; b) $\varepsilon = 0.05$; two different slices: Left: $\xi_y = 0$, like in a), Right: $\xi_y = 4 \cdot \Delta x$.*

Figure 4.7 displays comparisons of the position density $n(x, y, z = 0, t = 4)$ and evolution of the position density $n(x, 0, 0, t)$ for data 1 for the 4 different parameter regimes case I, III, IV and V, with $\varepsilon = 0.1$. Figure 4.8 shows the minimal difference of case I and II, with data 1 and $\varepsilon = 0.1$. Figure 4.9 is the analogue of Fig. 4.7 for the free Schrödinger evolution for data 1. Figure 4.10 displays a result for data 2.

The simulations of figure 4.7 show again that the critical scaling is at $\alpha = O(\sqrt{\varepsilon})$ - a careful examination of figure b) shows also a less regular behaviour than for c) and d). For $\alpha = O(\varepsilon^2)$ the figure is virtually the same as for $\alpha = 0$, so we skipped that plot and present Figure 4.8 only, where the minimal difference is visible. Hence in some physical situations, we can conclude that in case that the "local exchange term" occurs only at $O(\varepsilon^2)$ the effect of the Pauli principle can be neglected and the Schrödinger-Poisson model is sufficiently precise.

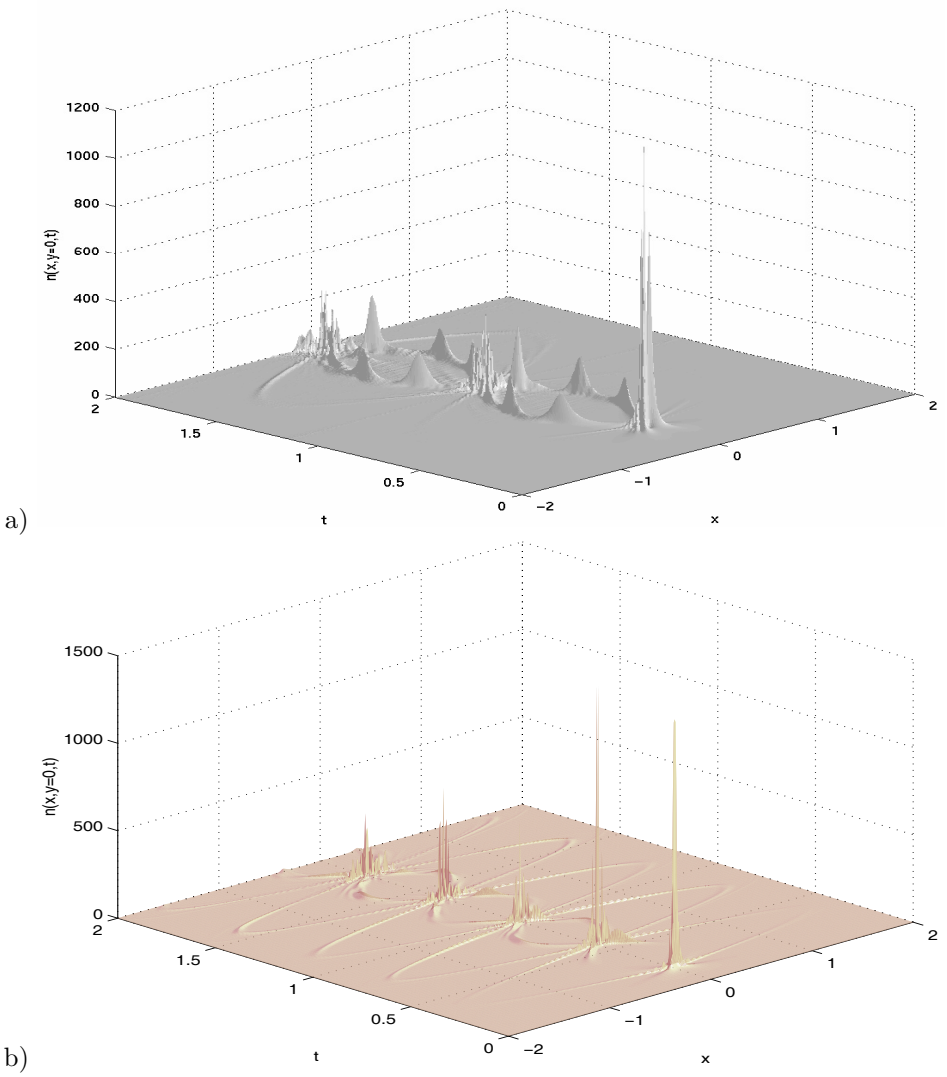

FIG. 4.6. *Evolution of position density of slice* $y = 0$ *in example 2 with case 3 initial data and* $\alpha = 0.5$, $C = 0$; $V_{\text{ext}} = \frac{\omega^2}{2}(x^2 + y^2)$, $\varepsilon = 0.04$. *a)* $\omega = 4$; *b)* $\omega = 8$.

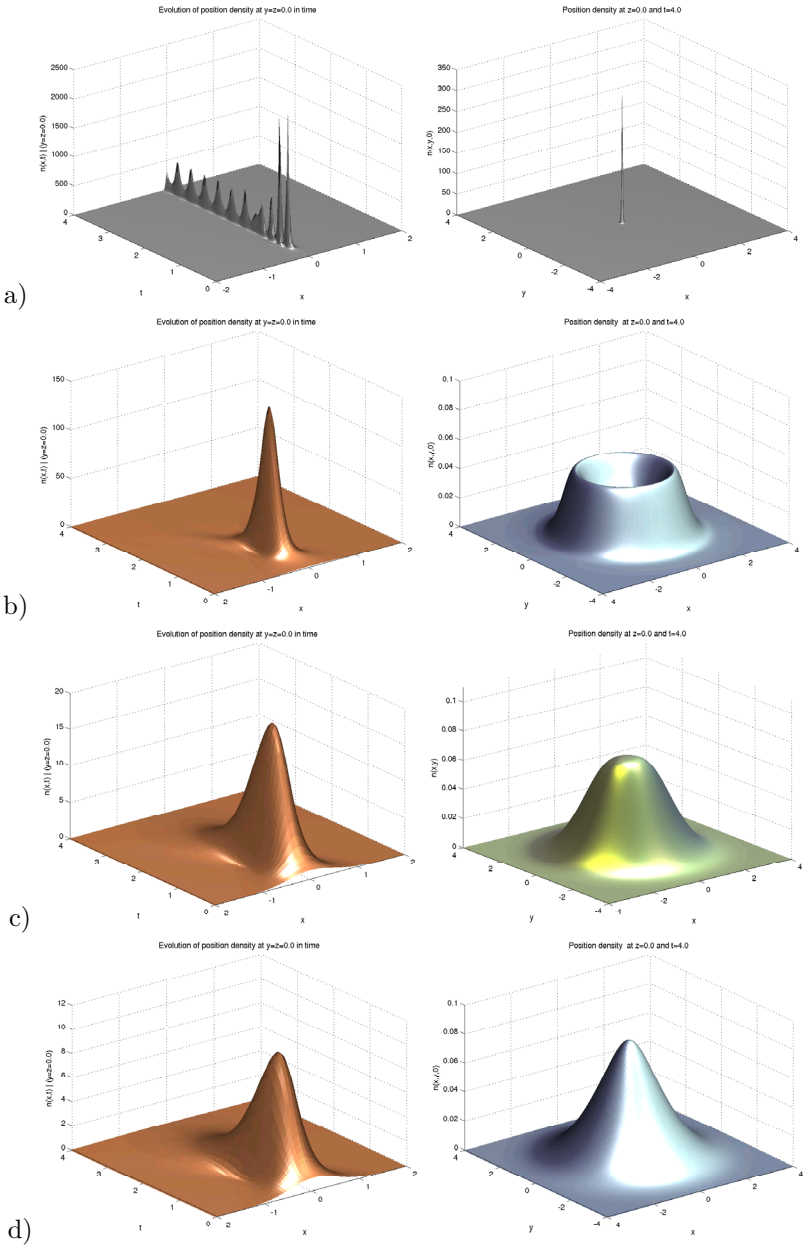

FIG. 4.7. *Numerical results for 3d S-P-Xα model in example 3 with* $C = 1$, $\varepsilon = 0.1$, $V_{\text{ext}} \equiv 0$ *for different regime of the parameter* α*; Left: Evolution of position density on* $y = z = 0$, *i.e.* $n(x, 0, 0, t)$*; Right: Position density at time* $t = 4$ *on* $z = 0$, *i.e.* $n(x, y, 0, t = 4)$. *a)* $\alpha = 1$ *; b)* $\alpha = \sqrt{\varepsilon}$*; c)* $\alpha = \varepsilon$*; d)* $\alpha = 0$.

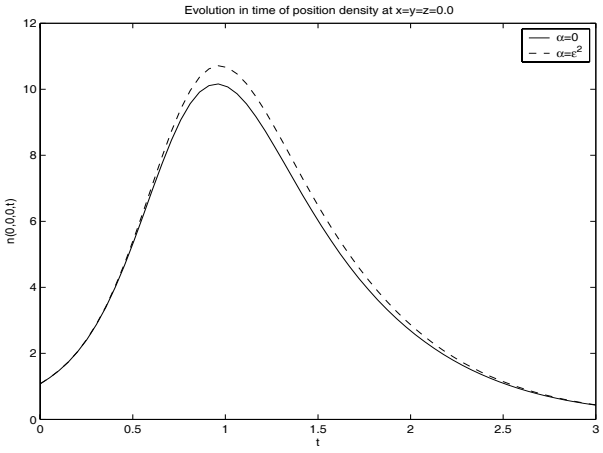

FIG. 4.8. *Evolution in time of position density at the origin* $(x, y, z) = (0, 0, 0)$. *Comparison of case I* ($\alpha = 0.0$) *and II* ($\alpha = \varepsilon^2$).

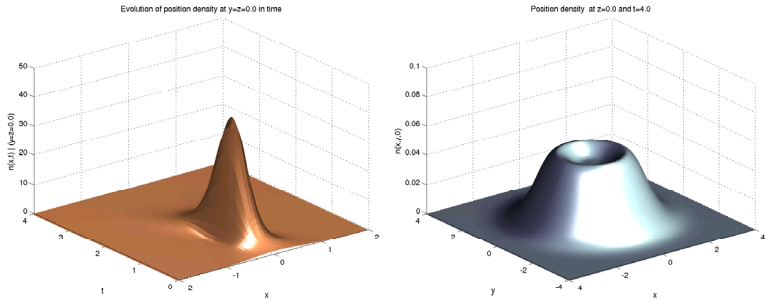

FIG. 4.9. *Numerical results for free 3d Schrödinger equation* ($C = 0$, $\alpha = 0$). *Same data as in Fig. 4.7:* $\varepsilon = 0.1$, $V_{\rm ext} \equiv 0$. *Left: Evolution of position density on* $y = z = 0$, *i.e.* $n(x, 0, 0, t)$; *Right: Position density at time* $t = 4$ *on* $z = 0$, *i.e.* $n(x, y, 0, t = 4.0)$.

In Figure 4.9 we show the evolution of the density for the "free" case, i.e. without any potential. Due to the nonzero "compressive" initial phase we have a formation of caustics also in this case and it is interesting that the pattern looks like something between the pattern in c) and b), i.e. of the full S-P-Xα model at $\alpha = O(\sqrt{\varepsilon})$.

In the last figure 4.10 we attempt to illustrate the complex pattern of the 3-d density after the break time by plotting the x-y plane for 2 values of z that are quite close. In some sense the rich soliton like structure of peaks that is proven to exist even analytically for the 1-d integrable NLS [MK] is occurring also in the 3-d system where such analytical results are missing.

5. Discussion

We present a first numerical study of the Schrödinger-Poisson-Xα (S-P-Xα) equation as a "local effective one particle approximation" of the time dependent Hartree-Fock equations. This particular NLS is the simplest model for quantum dynamics of electrons that respects the Pauli principle.

The S-P-Xα model (eventually including an external potential) is discretized by

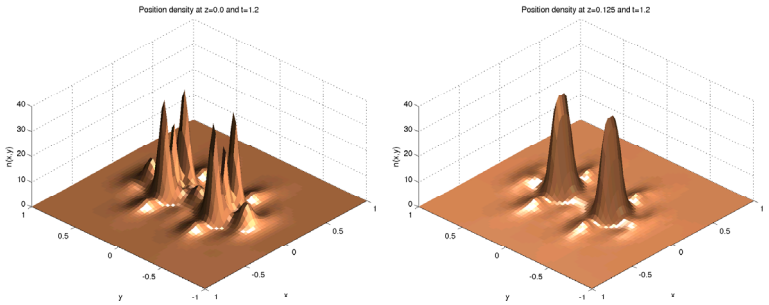

FIG. 4.10. *Asymmetric Data 2. Position density at* $t = 1.2$ *(post-break). Left:* $z = 0.0$*, Right:* $z = 0.125$*.* $\varepsilon = 0.075$*,* $\alpha = 1$*,* $C = 1$*,* $\Delta t = 0.01$*.*

a time-splitting spectral method. The merit of this numerical method is that it is explicit, unconditionally stable, time reversible and time transverse invariant and gives a 'good' ε-resolution for the S-P-Xα model in the semi-classical regime.

Extensive numerical results of position density and Wigner measures in 1, 2 and 3 space dimensions for the S-P-Xα model with/without an external potential are presented.

The interplay of the smoothing nonlocal nonlinearity - i.e. the repulsive "direct Coulomb interaction" ("Hartree potential") - with the strong local nonlinearity - i.e. the local approximation of the exchange interaction ("Xα potential")- is systematically studied by varying the scaling of the 2 nonlinearities between the Schrödinger-Poisson equation and an "exchange only" model. A critical scaling occurs when the Hartree term is $O(1)$ and the $X\alpha$ term is $O(\varepsilon)$.

In all simulations a critical time, the "break time", can be clearly distinguished and its "semiclassical limit" can be numerically estimated by comparing simulations with decreasing ε. Such simulations require a fine discretization which could be achieved also in 3-d by implementing the numerical code on a parallel machine.

The results in 1-d show a similarity to simulations of the "focusing cubic" NLS (as also studied in [BJM2]), with the smoothing effect of the additional Poisson equation nonlinearity. The well known "soliton" structure of the NLS (see e.g. [MK]) is preserved in the S-P-Xα model when the cubic nonlinearity is dominant.

In 3-d, our simulations show a similarity with simulations of Bose-Einstein-Condesates modeled by the time dependent Gross-Pitaevski equation, where the third root of the density of the S-P-Xα model is replaced by the density itself [BJaM], i.e. a cubic NLS. In both cases, the local nonlinearity has the "focusing sign". However, the additional smoothing effect of the Hartree potential and the lower exponent of the local nonlinearity show a somewhat "smoother" structure of the solution unless the $X\alpha$ term and the Hartree term are of the same order of magnitude.

6. Conclusion

We have shown that the $S - P - X\alpha$ model allows for simulations of quantum dynamics in 3 dimensions, also in the semiclassical regime. The inclusion of the exchange interaction to the widely used Schrödinger-Poisson model leads to qualitative changes in the transient behaviour of the solution that become very pronounced beyond a relative scaling of $O(\varepsilon)$ and change the behaviour completely towards the

typical "soliton-like structures" of the focusing cubic NLS beyond a relative scaling of $O(\sqrt{\varepsilon})$.

Acknowledgment. W.B. acknowledges support from the National University of Singapore and the Austrian Wittgenstein award of P.A. Markowich. N.J.M. and H.P.S. acknowledge financial support by the Austrian START award project "Nonlinear Schrödinger and Quantum Boltzmann equations" (grant number FWF Y-137-TEC) and by the European network "HYKE" (Contract Number: HPRN-CT-2002-00282).

REFERENCES

[Ba1] V. Bach, *Accuracy of mean field approximations for atoms and molecules*, Commun. Math. Phys., 155:295–310, 1993.

[B] J. Bourgain, *The nonlinear Schrödinger equation*, AMS, 1999.

[BaG] C. Bardos, F. Golse, and N.J. Mauser, *Weak coupling limit of the N-particle Schrödinger equation*, Mathematical Analysis and Applications, 7(2):275–293, 2000.

[BM2] C. Bardos, F. Golse, A. Gottlieb, and N.J. Mauser, *Mean field dynamics of fermions and the time-dependent Hartree-Fock equation*, J. d. Mathematiques Pures et Appl., 82(6):665–683, 2003.

[BM3] C. Bardos, A. Gottlieb, F. Golse, and N.J. Mauser, *Derivation of the time-dependent Hartree-Fock equation: the Coulomb interaction case*, manuscript.

[BMY] C. Bardos, L. Erdös, F. Golse, N.J. Mauser, and H.T. Yau, *Derivation of the Schrödinger-Poisson equation from the quantum N-particle Coulomb problem*, C. R. Acad. Sci., t. 334(6):515–520, Série I Math., 2002.

[BM1] O. Bokanowski and N.J. Mauser, *Local approximation for the Hartree-Fock exchange potential: a deformation approach*, Math.Meth., and Mod.in the Appl.Sci., 9(6):941–961, 1999.

[BGM] O. Bokanowski, B. Grébert, and N.J. Mauser, *Local density approximation for the energy of a periodic coulomb model*, Math.Meth., and Mod.in the Appl.Sci., 13(8):1185-1217, 2003.

[BJM1] W. Bao, S. Jin, and P.A. Markowich, *Time-splitting spectral approximations for the Schrödinger equation in the semiclassical regime*, J. Comp. Phys., 175(2):487–524, 2002.

[BJM2] W. Bao, S. Jin, P.A. Markowich, *Numerical studies of time-splitting spectral discretisations of nonlinear Schrödinger equations in the semiclassical regime*, SIAM J. Sci. Comp., 25(1):27–64, 2003,

[BJ] W. Bao and D. Jaksch, *An explicit unconditionally stable numerical method for solving damped nonlinear Schrödinger equations with a focusing nonlinearity*, SIAM J. Numer. Anal., 41(4):1406–1426, 2003.

[BJaM] W. Bao, D. Jaksch, and P.A. Markowich, *Numerical solution of the Gross-Pitaevskii equation for Bose-Einstein condensation*, J. Comput. Phys., 187(1):318–342, 2003.

[Caz] T. Cazenave, *Introduction to nonlinear Schrödinger equations*, Textos de Métodos Matemáticos 26, Rio de Janeiro, Instituto de Matemática-UFRJ, 1996.

[Car] R. Carles, *Remarques sur les mesures de Wigner*, Série I, 332:981–984, C.R.A.S. Paris, 2001.

[Co] J.W.D. Conolly, The $X\alpha$ method in *Semi-empirical methods of electronic structure calculations*, ed., by G.A. Segal, Plenum Press, 1977.

[D1] P.A.M. Dirac, *Note on exchange phenomena in the Thomas-Fermi atom*, Proc. Cambridge Philos. Soc., 26:376–385, 1931.

[G1] R. Gaspar, *Über eine approximation des Hartree-Fockschen potentials durch eine universelle Potentialfunktion*, Acta. Phys., Hungarica, 3:263–285, 1954.

[GMM] P. Gérard, P.A. Markowich, N.J. Mauser, and F. Poupaud, *Homogenization limits and Wigner transforms*, Comm. Pure and Appl. Math., 50:321–377, 1997.

[GV] J. Ginibre and G. Velo, *An introduction to nonlinear Schrödinger equations*, Hokkaido Univ., Technical Report Series in Math., 43:80–128, 1996.

[KPV] C. Kenig, G. Ponce, and L. Vega, *On the IVP for the nonlinear Schrödinger equations*, AMS Contemp. Math., 189:353–367, 1995.

[KS] W. Kohn and L.J. Sham, *Self-consistent equations including exchange and correlation effects*, Phys. Rev., A(140):1133, 1965.

[Lio1] P.L. Lions, *Solution of Hartree-Fock equations for Coulomb systems*, Comm. Math. Phys., 109:33–97, 1987.

[LP] P.L. Lions and T. Paul, *Sur les Mesures de Wigner*, Revista Mat. Iberoamericana, 9:553–618, 1993.

[M1] N.J. Mauser, *Quantum steady states: The Bloch-Poisson model*, Proc. "Numsim 91", Berlin, Ed., P. Deuflhard, Techn. Rep., 91–8, ZIB, 62–67, 1991.

[M2] N.J. Mauser, *The Schrödinger-Poisson-Xα model*, Appl. Math. Lett., 14:759–763, 2001.

[M3] N.J. Mauser, *(Semi)classical limits for weakly nonlinear Schrödinger equation*, Sem. Ecole Polytechnique, 1–12, 2002.

[MM1] P.A. Markowich and N.J. Mauser, *The Classical limit of a self–consistent quantum–vlasov equation in 3–D*, Math. Mod. and Meth. in Appl. Sciences, 9:109–124, 1993.

[MPPS] P.A. Markowich, P. Pietra, C. Pohl, and H.P. Stimming, *A Wigner-measure analysis of the Dufort-Frankel scheme for the Schrödinger equation*, SIAM J. Numer. Anal., 40(4):1281–1310, 2002.

[MPP] P.A. Markowich, P. Pietra, and C. Pohl, *A Wigner measure approach to the analysis of difference methods for the Schrödinger equation*, ENUMATH 97 (Heidelberg), 453–460, World Sci. Publishing, River Edge, NJ, 1998.

[MK] P. Miller and S. Kamvissis, *On the semiclassical limit of the focusing nonlinear Schrödinger equation*, Phys. Lett., A247(1-2):75–86, 1998.

[PY] R.G. Parr and W. Yang, *Density Functional Theory of Atoms and Molecules*, Oxford university press, 1989.

[Sla] J.C. Slater, *A simplification of the Hartree-Fock method*, Phys. Rev., 81(3):385–390, 1951.

[SSJM] E. Skovsen, H. Stapelfeldt, S. Juhl, and K. Molmer, *Quantum state tomography of dissociating molecules*, Phys. Rev. Lett., 91(9):406–410, 2003.

[Ste1] H. Steinrück, *The one-dimensional Wigner-Poisson problem and its relation to the Schrödinger-Poisson problem* SIAM J. Math. Anal., 22(4):957–972, 1991.

[Stim1] H.P. Stimming, *The IVP for the Schrödinger-Poisson-Xα equation in one dimension*, manuscript, 2003.

[WH] J.A.C. Weideman and B.M. Herbst, *Split-step methods for the solution of the nonlinear Schrödinger equation*, SIAM J. Numer. Anal., 23(3):485–507, 1986.

[ZZM] P. Zhang, Y. Zheng, and N.J. Mauser, *The limit from the Schrödinger-Poisson to Vlasov-Poisson equation with general data in one dimension*, Comm. Pure and Appl. Math., 55(5):582–632, 2002.